IEEE Access
Multidisciplinary | Rapid Review | Open Access Journal

Received August 26, 2019, accepted September 3, 2019, date of publication September 12, 2019, date of current version September 24, 2019.

Digital Object Identifier 10.1109/ACCESS.2019.2940691

The New Purity and Capacity Models for the OAM-mmWave Communication Systems Under Atmospheric Turbulence

HANQIONG LOU, XIAOHU GE, (Senior Member, IEEE), AND QIANG LI, (Member, IEEE)
School of Electronic Information and Communications, Huazhong University of Science and Technology, Wuhan 430074, China

Corresponding author: Qiang Li (qli_patrick@hust.edu.cn)

This work was supported in part by the National Key Research and Development Program of China under Grant 2016YFE0133000, and in part by the EU-China Study on the IoT and 5G under Grant EXCITING-723227.

ABSTRACT The orbital angular momentum (OAM) wireless communication technology is widely studied in recent literatures. But the atmospheric turbulence is rarely considered in analyzing the capacity of OAM-based millimeter wave (OAM-mmWave) communication systems. The OAM-mmWave propagated in the atmosphere environments is usually interfered by the atmospheric turbulence, resulting in the crosstalk among OAM channels, capacity degradation, etc. By taking into account the atmospheric turbulence effect, this paper proposes a new purity model and a new capacity model for the OAM-mmWave communication systems. Simulation results indicate that the OAM-mmWave propagation in the atmosphere environments is evidently interfered by atmospheric turbulence, where the capacity of the OAM-mmWave communication systems decreases with the increase of the transmission frequency.

INDEX TERMS Atmospheric turbulence, orbital angular momentum, millimeter wave, capacity.

I. INTRODUCTION

The electromagnetic waves have the linear momentum in the propagation directions and the angular momentum in the vertical planes of propagation directions. The angular momentum is classified by two types of angular moments, *i.e.*, the spin angular momentum (SAM) describing the electromagnetic wave polarization and the orbital angular momentum (OAM) describing the electromagnetic wave spiral phase [1]. The SAM has only two mutually orthogonal states, the OAM has an infinite number of orthogonal states that can be multiplexed along the same propagation axis. Thus, the OAM can be used for improving the signal transmission efficiency without additional frequency band occupancy [2].

When the OAM technology is adopted for optical communications, the transmission capacity has been obviously improved [3]–[6]. However, in the presence of atmospheric turbulence, the phase of optical waves carrying OAM could be changed, which decreases the capacity of OAM wireless communication systems seriously [7]–[9]. The propagation characteristics of OAM light waves considering atmospheric turbulence have been investigated in [10], [11]. Due to the atmospheric turbulence, the energy of the transmitted OAM state spread into neighboring OAM states with different probabilities, which resulted in crosstalk in OAM-Multiplexed free space optical communication systems [10]. The crosstalk model of OAM-Multiplexed free space optical communication systems with the atmospheric turbulence effect was used for selecting the optimal set of OAM states to maximize the capacity of OAM communication systems [11]. The spiral spectrum of OAM light waves in Kolmogorov turbulence was researched in [12]. Then the spiral spectrum of OAM beam in non-Kolmogorov turbulence was also studied in [13].

In recent years, the OAM technology has been used to improve the capacity of wireless communications [16]–[19]. However, the impact of the atmosphere effect on the OAM wireless communications using radio is rarely investigated [20]–[24]. Therefore, it is of significant importance to evaluate the impact of atmospheric turbulence on the capacity of OAM wireless communication systems. Considering the directional characteristic of OAM waves, the capacity of OAM-multiplexed communication systems with unaligned transceiver antenna arrays was shown to be

The associate editor coordinating the review of this manuscript and approving it for publication was Cunhua Pan.

smaller than the capacity of OAM-multiplexed communication systems with aligned transceiver antenna arrays [20]. Because the OAM waves could decrease the spatial correlation of wireless channels, the capacity of OAM-based Multiple-Input Multiple-Output (MIMO) systems was shown to be larger than the capacity of the traditional MIMO systems in free space with weak multipath effect [21]. Moreover, the energy efficiency of OAM spatial modulation millimeter wave communication systems was shown to be higher than the energy efficiency of OAM-based MIMO systems [22], which made OAM spatial modulation millimeter wave communication systems more suitable for transmissions in long distances efficiently. In view of the fact that the divergence of OAM-based radio vortex waves is more significant than the divergence of radio plane waves, a new type of bifocal lens antenna was used for transmitting OAM-based signals to reduce the propagation attenuation [23]. However, in these studies, only Gaussian white noise was considered as the external interference factor in the OAM wireless propagation. An interesting problem arises as to whether the influence of atmospheric turbulence on the OAM wave transmissions is the same as the influence of atmospheric turbulence on the OAM millimeter wave (OAM-mmWave) transmissions.

In this paper the impact of atmospheric turbulence on the OAM-mmWave communication systems has been investigated. A new capacity model has been proposed for the OAM-mmWave communication systems considering the atmospheric turbulence effect. The contributions of this paper are summarized as follows:

1) A new purity model is proposed for OAM-mmWave communication systems considering the propagation characteristics of OAM-mmWave with the atmospheric turbulence. In general, the atmospheric turbulence causes the power of the transmitted OAM state to spread into the adjacent OAM states, *i.e.*, the crosstalk effect of atmospheric turbulence.
2) A capacity model is proposed for the OAM-mmWave communication systems based on the atmospheric turbulence. The crosstalk among channels with different OAM states is characterized based on the proposed capacity model.
3) Conventionally, without considering the atmospheric turbulence, the capacity of OAM-mmWave communication systems is found to be irrelevant to the transmission frequency. By contrast, in this paper simulation results show that the capacity of OAM-mmWave communication systems, in the presence of the atmospheric turbulence, decreases with the increase of the transmission frequency. Moreover, simulation results indicate that the capacity of OAM-mmWave communication systems decreases with the increase of the refractive index structure constant that is proportional to the atmospheric turbulence intensity.

The rest of this paper is organized as follows. In Section II, a new purity model is established for the OAM millimeter waves considering the atmospheric turbulence.

TABLE 1. A list of symbols appear in this paper.

Symbol	Quantity
$u_{p,l}(r,\phi,z)$	field distribution of the OAM wave
(r,ϕ,z)	cylindrical coordinate system
z	propagation distance
α	arbitrary complex constant
i	imaginary unit
p	radial index
$w(z)$	beam waist radius of the OAM wave
w_0	beam waist radius at z = 0
$R(z)$	phase front radius of curvature of LG beam at receiver
z_R	Rayleigh distance
λ	wavelength
f	frequency
k	wave number
l_0, m	transmitted OAM state
l, n	received OAM state
r_0	spatial coherence radius of the LG beam wave
Θ	curvature parameter of the LG beam at receiver
Λ	Fresnel ratio of the LG beam at receiver
C_n^2	refractive index structure constant
$u(r,\phi,z)$	field distribution in atmosphere environments
$P_{l_0}(l_0,z)$	purity of the millimeter wave with OAM state l_0
$P_l(l_0,z), P_n(m,z)$	power weight of the spiral harmonic component
L	the number of OAM channels
S	transmitted OAM state set
$\mathbf{P}$	crosstalk matrix of OAM channels
Υ	signal to-interference-and-noise ratio matrix
N_0	additive white Gaussian noise power
P_{TX}	transmitted power
$\mathbf{p}$	bit error rate matrix of OAM channels
$\mathbf{C_L}$	capacity matrix of OAM channels
C	capacity of the communication system
C_{ideal}	capacity of the ideal communication system

In Section III, the capacity model for OAM-mmWave communication systems with the atmospheric turbulence is proposed. In Section IV, the simulation results are analyzed and discussed. Finally, conclusions are drawn in Section V.

II. PURITY MODEL BASED ON ATMOSPHERIC TURBULENCE

A. SYSTEM MODEL

As shown in Fig.1, due to the diffractive effect, the propagation of OAM waves is divergent in the free space and the intensity of OAM waves is mainly distributed in the annular region [11]. In this paper the Laguerre-Gaussian (LG) beam is used to describe the OAM wave. Hence, the field distribution

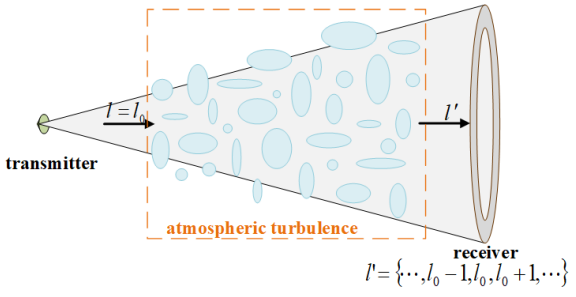

FIGURE 1. An illustration of the OAM-mmWave propagation in the atmosphere environment.

of the OAM wave is expressed in cylindrical coordinate system (r, ϕ, z) as [25]

$$u_{p,l}(r,\phi,z) = \alpha\sqrt{\frac{p!}{\pi\,(p+|l|)!}}\frac{1}{w(z)}\left(\frac{\sqrt{2}r}{w(z)}\right)^{|l|}e^{-\left(\frac{r}{w(z)}\right)^2} \times L_p^{|l|}\left(\frac{2r^2}{w^2(z)}\right)e^{\frac{-i\pi r^2}{\lambda R(z)}}e^{i(|l|+2p+1)\zeta(z)}e^{-il\phi}, \tag{1a}$$

with

$$w(z) = w_0\sqrt{1+\left(\frac{z}{z_R}\right)^2}, \tag{1b}$$

$$R(z) = z\left[1+\left(\frac{\pi w_0^2}{\lambda z}\right)^2\right], \tag{1c}$$

where r is radial distance, ϕ is azimuthal angle, z is propagation distance, α is an arbitrary complex constant, i is an imaginary unit, p is the radial index, $p = 0$ is generally configured for OAM systems. l is the OAM state, $l \in \{+|l|, -|l|\}$. The rotation direction of the spiral wavefront is determined by the symbol of l. The absolute value of l represents the number of equiphase surfaces wound on the propagation axis. When $l = 0$, the electromagnetic wave is a conventional plane wave or spherical wave. $w(z)$ is the beam waist radius of the OAM electromagnetic wave at the propagation distance z. w_0 is the beam waist radius at $z = 0$. $\zeta(z) = \arctan\left(\frac{z}{z_R}\right)$ is the Gouy phase, where $z_R = \frac{\pi w_0^2}{\lambda}$ is the Rayleigh distance, λ is the wavelength. f is the frequency. $L_p^{|l|}\left(\frac{2r^2}{w^2(z)}\right)$ is a generalized Laguerre polynomial, $L_p^{|l|}\left(\frac{2r^2}{w^2(z)}\right) = 1$ when $p = 0$. The propagation characteristics of OAM waves in the millimeter wave band are studied in this paper. The equiphase surface of the LG beam is a spiral with the curvature radius $R(z)$, which is formulated by (1c). The intensity of OAM waves is mainly distributed in an annular region, where the radius of the ring with the maximum intensity is derived by [24]

$$r_{\max}(z) = \sqrt{\frac{|l|}{2}}w(z). \tag{2}$$

This is a key factor that directly affects the choice of receiver radius. The radius of receiver is large than $r_{\max}(z)$. Because the wavelength of the millimeter wave is longer than the wavelength of light, based on (2), the divergence degree of the OAM-mmWave is larger than the divergence degree of the OAM light wave at the same distance. Due to the practical consideration of the receiver, the propagation distance of the OAM-mmWave is limited.

In the actual atmosphere environments, the atmospheric turbulence interferes with the propagation of OAM-mmWaves and causes the power of the emitted OAM states to spread into the adjacent OAM states. After the OAM-mmWave with the OAM state l_0 is transmitted in atmosphere environments, the OAM-mmWaves with the OAM state $l \in \{\cdots, l_0-1, l_0, l_0+1, \cdots\}$ are received at the receiver. In this paper, the Kolmogorov turbulence model is used to approximate the atmospheric turbulence interferences in OAM-mmWave propagation. Considering the Kolmogorov turbulent flow, the spatial coherence radius of the LG beam wave is expressed as [31]

$$r_0 = \left[\frac{8}{3\left(a+0.618\Lambda^{\frac{11}{6}}\right)}\right]^{\frac{3}{5}}(1.46C_n^2k^2z)^{-\frac{3}{5}}, \tag{3a}$$

with

$$a = \frac{1-\Theta^{\frac{8}{3}}}{1-\Theta}, \tag{3b}$$

$$\Lambda = \frac{2z}{k\omega^2(z)}, \tag{3c}$$

where $k = 2\pi/\lambda$ is the wave number, $\Theta = 1 + \frac{z}{R(z)}$ is the curvature parameter of the LG beam at receiver, Λ is the Fresnel ratio of the LG beam at receiver, C_n^2 is the refractive index structure constant. Turbulence strength increases with the increase of C_n^2 [11]. In near-surface environments, C_n^2 is affected by temperature and humidity. The key influencing factor of C_n^2 in the optical band is temperature. The key influencing factor of C_n^2 in the millimeter wave band is humidity [27], [29]. Hence, the value of C_n^2 is related to the frequency when the environmental conditions are the same. The C_n^2 of the millimeter waves is two orders of magnitude larger than the C_n^2 of the light waves [27]. When the millimeter wave band is adopted for OAM propagations, the statistical average of C_n^2 is $4.0 \times 10^{-12}\mathrm{m}^{-\frac{2}{3}}$ in near-surface environments [29].

At present, the research on OAM-mmWave communication systems generally only considers white Gaussian noise. In this case, the orthogonality of OAM-mmWave states is maintained for the propagation of OAM-mmWave [24], [25]. But the atmospheric turbulence causes the phase distortion and the loss of orthogonality in the actual atmosphere environments. In order to describe this phenomenon theoretically, it is necessary to calculate the purity model of OAM millimeter wave according to the Kolmogorov turbulence model.

B. PURITY MODEL

In the actual atmosphere environments, the atmospheric turbulence causes the phase distortion and intensity fading in OAM-mmWave propagation [34]. Based on the measured results, the value of intensity fading is small in most atmospheric turbulence scenarios [15], [35]. Considering that this paper focuses on the phase distortion due to the atmospheric turbulence, the intensity fading is ignored in this paper. In this case, the orthogonality of OAM-mmWave states can't be maintained for the propagation of OAM-mmWave in atmosphere environments. Therefore, it is necessary to analyze the propagation characteristics of OAM-mmWave with the atmospheric turbulence.

Applying the Rytov approximation, the phase distortion of spherical wave caused by the atmospheric turbulence is

expressed as [31]

$$u(r,\phi,z) = u_{p,l_0}(r,\phi,z)e^{\psi(r,\phi,z)}. \tag{4a}$$

Based on the quadratic approximation [31], $\psi(r,\phi,z)$ satisfies

$$\left\langle e^{\psi(r,\phi,z)+\psi^*(r,\phi',z)}\right\rangle = e^{\frac{2r^2}{r_0^2}(\cos(\phi'-\phi)-1)}. \tag{4b}$$

Because multiple spherical waves with different phases can be used to generate an OAM wave [42], [43], the Rytov approximation and quadratic approximation of spherical waves can be used for OAM waves.

When the atmospheric turbulence is considered for the OAM wave propagation, the power of the emitted OAM state spreads into the adjacent OAM states [14]. $e^{-il\phi}$ represents the helical phase distribution, so (1a) can be written as

$$u_{p,l}(r,\phi,z) = \frac{1}{\sqrt{2\pi}}a_l(r,z)e^{-il\phi}, \tag{5a}$$

with

$$a_l(r,z) = \alpha\sqrt{\frac{2p!}{(p+|l|)!}}\frac{1}{w(z)}\left(\frac{\sqrt{2}r}{w(z)}\right)^{|l|}e^{-\left(\frac{r}{w(z)}\right)^2} \times L_p^{|l|}\left(\frac{2r^2}{w^2(z)}\right)e^{\frac{-i\pi r^2}{\lambda R(z)}}e^{i(|l|+2p+1)\zeta(z)}. \tag{5b}$$

In this case the field strength of the OAM-mmWave in (4a) is expanded into multiple OAM states (The OAM states interval is $(-\infty,+\infty)$). Therefore, (4a) can be rewritten as

$$u(r,\phi,z) = \frac{1}{\sqrt{2\pi}}\sum_{l=-\infty}^{\infty}a_l(r,z)e^{-il\phi}. \tag{6}$$

According to the discrete-time Fourier transform, the coefficient $a_l(r,z)$ is expressed as

$$a_l(r,z) = \frac{1}{\sqrt{2\pi}}\int_0^{2\pi}u(r,\phi,z)e^{il\phi}d\phi. \tag{7}$$

The power weight of the spiral harmonic component with OAM state l is expressed as

$$P_l(l_0,z) = D_l(l_0,z)/\sum_{n=-\infty}^{\infty}D_n(l_0,z), \tag{8a}$$

with $D_l(l_0,z)$ given in (8b), shown at the bottom of this page, where $\left\langle|a_l(r,z)|^2\right\rangle$ represents the probability density distribution of OAM-mmWave with state l, $\int_0^{2\pi}e^{-in\phi'+\eta\cos(\phi'-\phi)}d\phi' = 2\pi e^{-in\phi}I_n(\eta)$ [41], $I_n(\cdot)$ is the modified n-order Bessel function of the first kind, R is the radius of receiver. Purity is defined as the proportion of the original state power in the total power of the OAM-mmWaves after the propagation in atmosphere environments [32]. From the definition of purity, it is known that $P_{l_0}(l_0,z)$ is the purity of the millimeter wave with OAM state l_0.

The undistorted electric field of (1a) at $z=0$ is given as

$$u_{p,l_0}(r,\phi,0) = \frac{1}{\sqrt{2\pi}}\beta_{l_0}(r,0)e^{-il_0\phi}. \tag{9}$$

When $z=0$, $\sum_{n=-\infty}^{\infty}D_n(l_0,z)$ is denoted as the $D_{initial}$, which is expressed by

$$\begin{aligned}D_{initial} &= \int_0^R\left\langle\left|\beta_{l_0}(r,0)\right|^2\right\rangle rdr \\ &= 2\alpha^2\times\frac{p!}{(p+|l_0|)!}\times\frac{1}{w_0^2} \\ &\quad\times\int_0^R\left(\frac{2r^2}{w_0^2}\right)^{|l_0|}e^{\frac{-2r^2}{w_0^2}}\left[L_p^{|l_0|}\left(\frac{2r^2}{w_0^2}\right)\right]^2 rdr.\end{aligned} \tag{10}$$

When the OAM-mmWave power weight is normalized by $D_{initial}$, the power weight of the spiral harmonic component with OAM state l is given by (11), as shown at the top of the next page. When $l=l_0$ in (11), the purity $P_{l_0}(l_0,z)$ of the millimeter wave with OAM state l_0 is derived by (12), as shown at the top of the next page.

In order to make full use of the orthogonality of OAM-mmWave states, OAM-mmWave communication systems usually have multiple OAM waves with different OAM states for propagation simultaneously. Therefore, it is necessary to analysis the signal power crosstalk among adjacent OAM states according to the purity formula and obtain the capacity model of the OAM-mmWave communication system considering atmospheric turbulence.

$$\begin{aligned}D_l(l_0,z) &= \int_0^R\left\langle|a_l(r,z)|^2\right\rangle rdr \\ &= \frac{1}{2\pi}\int_0^R\int_0^{2\pi}\int_0^{2\pi}\left\langle u(r,\phi,z)u^*(r,\phi',z)\right\rangle e^{il(\phi-\phi')}d\phi d\phi' rdr \\ &= \frac{1}{2\pi}\int_0^R\int_0^{2\pi}\int_0^{2\pi}u_{p,l_0}(r,\phi,z)u_{p,l_0}^*(r,\phi',z)\left\langle e^{\psi(r,\phi,z)+\psi^*(r,\phi',z)}\right\rangle e^{il(\phi-\phi')}d\phi d\phi' rdr \\ &= \frac{\alpha^2w^{-2}(z)p!}{2\pi^2(p+|l_0|)!}\int_0^R\left(\frac{2r^2}{w^2(z)}\right)^{|l_0|}e^{-\frac{2r^2}{w^2(z)}-\frac{2r^2}{r_0^2}}\left[L_p^{|l_0|}\left(\frac{2r^2}{w^2(z)}\right)\right]^2\int_0^{2\pi}\int_0^{2\pi}e^{i(l-l_0)(\phi-\phi')}e^{\frac{2r^2\cos(\phi-\phi')}{r_0^2}}d\phi d\phi' rdr \\ &= \frac{2\alpha^2w^{-2}(z)p!}{(p+|l_0|)!}\int_0^R\left(\frac{2r^2}{w^2(z)}\right)^{|l_0|}e^{-\frac{2r^2}{w^2(z)}-\frac{2r^2}{r_0^2}}\left[L_p^{|l_0|}\left(\frac{2r^2}{w^2(z)}\right)\right]^2 I_{l-l_0}\left(\frac{2r^2}{r_0^2}\right)rdr\end{aligned} \tag{8b}$$

$$P_l(l_0,z)=\frac{D_l(l_0,z)}{D_{initial}}=\frac{\int_0^R\left(\frac{2r^2}{w^2(z)}\right)^{|l_0|}e^{-\frac{2r^2}{w^2(z)}-\frac{2r^2}{r_0^2}}\left[L_p^{|l_0|}\left(\frac{2r^2}{w^2(z)}\right)\right]^2 I_{l-l_0}\left(\frac{2r^2}{r_0^2}\right)rdr}{\frac{w^2(z)}{w_0^2}\int_0^R\left(\frac{2r^2}{w_0^2}\right)^{|l_0|}e^{-\frac{2r^2}{w_0^2}}\left[L_p^{|l_0|}\left(\frac{2r^2}{w_0^2}\right)\right]^2 rdr} \tag{11}$$

$$P_{l_0}(l_0,z)=\frac{D_{l_0}(l_0,z)}{D_{initial}}=\frac{\int_0^R\left(\frac{2r^2}{w^2(z)}\right)^{|l_0|}e^{-\frac{2r^2}{w^2(z)}-\frac{2r^2}{r_0^2}}\left[L_p^{|l_0|}\left(\frac{2r^2}{w^2(z)}\right)\right]^2 I_0\left(\frac{2r^2}{r_0^2}\right)rdr}{\frac{w^2(z)}{w_0^2}\int_0^R\left(\frac{2r^2}{w_0^2}\right)^{|l_0|}e^{-\frac{2r^2}{w_0^2}}\left[L_p^{|l_0|}\left(\frac{2r^2}{w_0^2}\right)\right]^2 rdr} \tag{12}$$

III. CAPACITY MODEL BASED ON ATMOSPHERIC TURBULENCE

The orthogonality among OAM states can be used to simultaneously transmit information by the wave of OAM-mmWave communication systems with the same frequency. As a consequent, electromagnetic waves multiplexing with different OAM states can be regarded as different channels in OAM-mmWave communication systems, *i.e.*, an OAM state is regarded as an OAM channel. The OAM state set transmitted by the transmitter is assumed as S. When the OAM-mmWave is propagated in atmosphere environments, the atmospheric turbulence results in the signal power crosstalk among adjacent OAM states for OAM-mmWave communication systems. In this case, the received signal power at the $n-th$ OAM channel is not only from the OAM-mmWave with the state n but also from the OAM-mmWaves with different states. When the OAM-mmWave communication system has $L=2N+1$ symmetrically distributed OAM channels *i.e.*, $S=\{-N,-N+1,\cdots,0,\cdots,N-1,N\}$, the crosstalk matrix of the OAM-mmWave communication system is expressed as (13),

$$\mathbf{P}=\begin{bmatrix} P_{-N}(-N,z) & \cdots & P_n(-N,z) & \cdots & P_N(-N,z)\\ \vdots & \ddots & \vdots & \ddots & \vdots\\ P_{-N}(m,z) & \cdots & P_n(m,z) & \cdots & P_N(m,z)\\ \vdots & \ddots & \vdots & \ddots & \vdots\\ P_{-N}(N,z) & \cdots & P_n(N,z) & \cdots & P_N(N,z)\end{bmatrix} \tag{13}$$

where $P_n(m,z)$, $-N\leqslant n\leqslant N$, $-N\leqslant m\leqslant N$ is the power weight of the spiral harmonic component with OAM state n, when the OAM-mmWave with the OAM state m is transmitted in atmosphere environments. When $l=n$, $l_0=m$, $m\neq n$ are substituted into (11), $P_n(m,z)$ represents that the normalized power is spread from the state m into the state n. The $m-th$ row of the matrix $\mathbf{P}$ describes that the normalized wave power of the $m-th$ OAM channel is spread into OAM channels which are included in the set S. The $n-th$ column of the matrix $\mathbf{P}$ includes the desired wave power of $n-th$ OAM channel and the spread wave power from other OAM channels which are included in the set S. Based on each column of the crosstalk matrix $\mathbf{P}$, the signal-to-interference-and-noise ratio (SINR) of OAM channels is expressed as

$$\Upsilon=[\,\gamma_{-N}\quad\cdots\quad\gamma_n\quad\cdots\quad\gamma_N\,], \tag{14a}$$

with

$$\gamma_n=\frac{P_n(n,z)}{\sum\limits_{\substack{m\in S\\ m\neq n}}P_n(m,z)+\frac{N_0}{P_{TX}}}, \tag{14b}$$

where γ_n is the SINR of the $n-th$ OAM channel, N_0 is the additive white Gaussian noise power, P_{TX} is the transmitted power. When the OAM-mmWave communication systems apply the orthogonal modulation, the bit error rate of OAM channels is derived as

$$\mathbf{p}=\left[\,p_{-N}\quad\cdots\quad p_n\quad\cdots\quad p_N\,\right], \tag{15a}$$

with [11]

$$p_n=\frac{1}{2}erfc\left(\sqrt{\frac{\gamma_n}{2}}\right), \tag{15b}$$

where p_n is the bit error rate of the $n-th$ OAM channel, $erfc(\cdot)$ is the complementary error function. It must be noted that the calculation of the bit error rate is related to the modulation formats. Moreover, even the same kind of modulation format such as M-QAM has different bit error rate when the M takes different values. 5-QAM and 9-QAM have better crosstalk tolerance than regular 4-QAM and 8-QAM, because 5-QAM and 9-QAM contains zero-power symbols which do not interfere with the symbols of adjacent channels [36]. The capacity of OAM channels is derived by

$$\mathbf{C_L}=\left[\,C(p_{-N})\quad\cdots\quad C(p_n)\quad\cdots\quad C(p_N)\,\right], \tag{16a}$$

with [11]

$$C(p_n)=1+p_n\log_2 p_n+(1-p_n)\log_2(1-p_n). \tag{16b}$$

With the assumption that each OAM channel is a binary symmetric channel, $C(p_n)$ is the capacity of the $n-th$ OAM channel. Based to (14b), $\sum\limits_{\substack{m\in S\\ m\neq n}}P_n(m,z)$ which represents the normalized wave power spread from other OAM channels is configured as independent each other. Therefore, the capacity of the OAM-mmWave communication system based on atmospheric turbulence is [7]

$$C=\sum_{n\in S}C(p_n), \tag{17}$$

which is the row sum of the matrix $\mathbf{C_L}$ in (16a).

TABLE 2. Default values of parameters.

default parameter	value
beam waist radius w_0	0.01m
propagation distance z	100m
transmission frequency f	100GHz
refractive index structure constant C_n^2	1×10^{-12} m$^{-\frac{2}{3}}$
signal-to-noise ratio SNR_0	10dB
receiver radius R	50m

In the ideal free space, there is no crosstalk among OAM channels with different OAM states, *i.e.*, $P_n(m,z) = 0$ when $n \neq m$ and $P_n(m,z) = 1$ when $n = m$. In this case, the SINR of each OAM channel satisfies $\gamma = P_{TX}/N_0$. As a consequent, the capacity of the ideal OAM-mmWave communication system without atmospheric turbulence is derived as

$$C_{ideal} = \frac{L}{2} erfc\left(\sqrt{\frac{P_{TX}}{2N_0}}\right) \log_2\left(\frac{1}{2} erfc\left(\sqrt{\frac{P_{TX}}{2N_0}}\right)\right) + L + \left(L - \frac{L}{2} erfc\left(\sqrt{\frac{P_{TX}}{2N_0}}\right)\right) \times \log_2\left(1 - \frac{1}{2} erfc\left(\sqrt{\frac{P_{TX}}{2N_0}}\right)\right). \quad (18)$$

IV. SIMULATION RESULTS AND DISCUSSIONS

The capacity model of OAM-mmWave communication systems considering the atmospheric turbulence is analyzed in this section. The OAM-mmWave communication system has $L = 2N + 1$ symmetrically distributed OAM states. The OAM state set transmitted by the transmitter is $S = \{-N, -N+1, \cdots, 0, \cdots, N-1, N\}$. $SNR_0 = 10 \times \lg(P_{TX}/N_0)$ is the signal-to-noise ratio. Default values of simulation parameters are set as follows: the beam waist radius $w_0 = 0.01$m, the propagation distance $z = 100$m, the transmission frequency $f = 100$GHz, the refractive index structure constant $C_n^2 = 1 \times 10^{-12}m^{-\frac{2}{3}}$, the signal-to-noise ratio $SNR_0 = 10$dB, the radius of receiver $R = 50m$.

Fig. 2 manifests that the power of the emitted OAM state spreads into the adjacent OAM states. The emitted OAM state is 10. Because of atmospheric turbulence, the power weight of OAM-mmWave with state 10 is 73.67%. The power weight of OAM-mmWave with state 9 is 12.01%. The power weight of OAM-mmWave with state 11 is 12.01%. The power weight of OAM-mmWave with state 8 is 1.08%. The power weight of OAM-mmWave with state 12 is 1.08%. The power weight of the other OAM states is very small. Most of the power remains in the emitted OAM state. The closer the OAM state is to the emitted OAM state, the higher its energy weight is.

Fig. 3 illustrates the impact of the number of OAM states on the capacity of OAM-mmWave communication systems with different transmission frequencies. When the transmission frequency effect is ignored in OAM-mmWave communication systems, i.e., the atmospheric turbulence effect

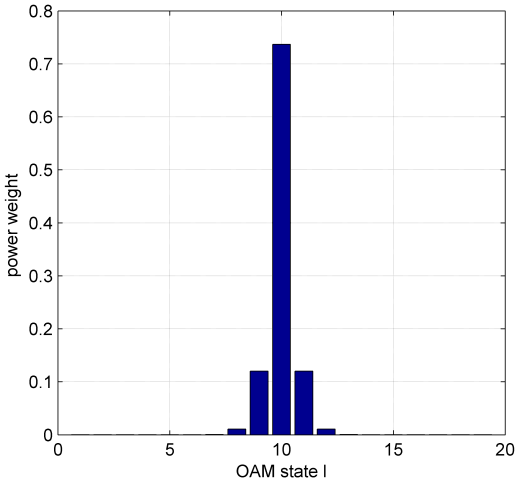

FIGURE 2. The power weight of the emitted OAM state spread into the adjacent OAM states.

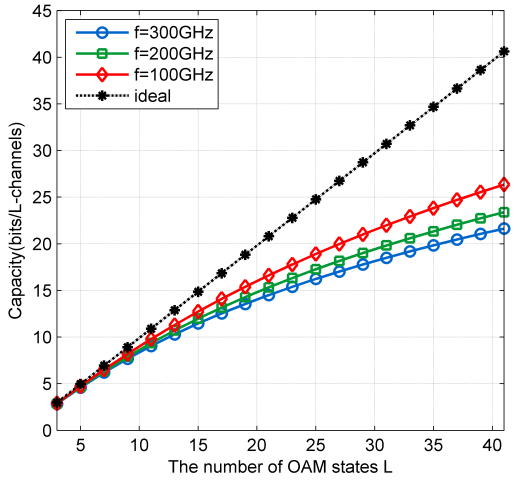

FIGURE 3. Impact of the number of OAM states on the capacity of OAM-mmWave communication systems with different transmission frequencies.

is ignored, the capacity of the ideal OAM-mmWave communication system based on (18) is plotted by the black dashed line in Fig. 3. When the transmission frequency is fixed, the capacity of OAM-mmWave communication systems increases with the increase of the number of OAM states. When the number of OAM states is fixed, the capacity of OAM-mmWave communication systems decreases with the increase of the transmission frequency. Moreover, the capacity of OAM-mmWave communication systems considering the atmospheric turbulence is less than the capacity of ideal OAM-mmWave communication systems.

Fig. 4 shows the impact of the number of OAM states on the capacity of OAM-mmWave communication systems with different refractive index structure constants. When the number of OAM states is fixed, the capacity of OAM-mmWave communication systems decreases with the increase of the refractive index structure constants which are proportional to the atmospheric turbulence intensity.

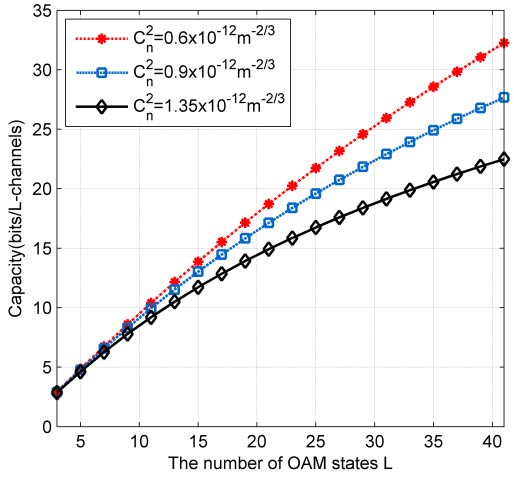

FIGURE 4. Impact of the number of OAM states on the capacity of OAM-mmWave communication systems with different refractive index structure constants.

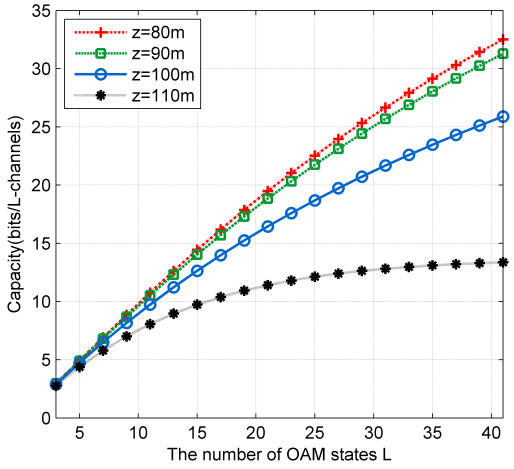

FIGURE 5. Impact of the number of OAM states on the capacity of OAM-mmWave communication systems with different propagation distances.

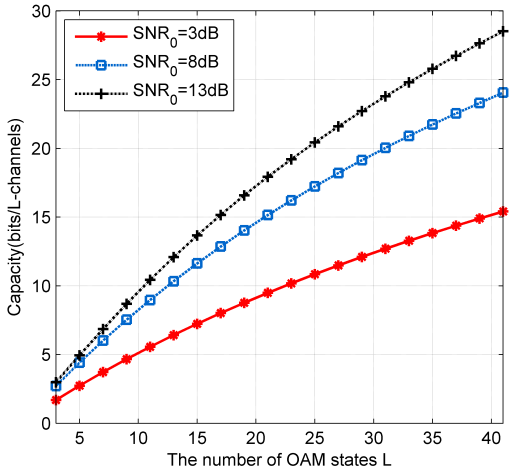

FIGURE 6. Impact of the number of OAM states on the capacity of OAM-mmWave communication systems with different SNR_0 values.

Fig. 5 describes the impact of the number of OAM states on the capacity of OAM-mmWave communication systems with different propagation distances. When the number of OAM states is fixed, the capacity of OAM-mmWave communication systems decreases with the increase of the propagation distance.

Fig. 6 depicts the impact of the number of OAM states on the capacity of OAM-mmWave communication systems with different SNR_0 values. When the number of OAM states is fixed, the capacity of OAM-mmWave communication systems increases with the increase of the SNR_0 values.

V. CONCLUSION

In conventional studies on OAM wireless communications, the atmospheric turbulence is rarely considered for analyzing the capacity of OAM-mmWave communication systems. By taking into account the effect of atmospheric turbulence, this paper proposes a new purity model and a new capacity model for the OAM-mmWave communication systems. When the atmospheric turbulence effect is ignored in conventional OAM wireless communication systems in most exiting works, the impact of transmission frequency on the OAM-mmWave communication systems is also ignored. However, simulation results of this paper show that the capacity of OAM-mmWave communication systems considering the atmospheric turbulence effect decreases with the increase of the transmission frequency. This paper provides guidelines for designing practical OAM-mmWave communication systems under the influence of atmospheric turbulence. The future research direction of this paper is to analyze the OAM-mmWave communication system model under Non-Kolmogorov turbulence model which is more accurate than Kolmogorov turbulence model to describe the real turbulence environment.

Various methods for mitigating the effect of atmospheric turbulence on OAM waves have been proposed in the optical band, such as MIMO equalization [37], adaptive optics [38], channel coding [40]. MIMO equalization can effectively improve the OAM signal quality and reduce the bit error rate in atmospheric turbulence. It is more suitable for mitigating the effect of weak atmospheric turbulence. Adaptive optics compensates for the effect of turbulence by using data-carrying Gaussian beacons. But it requires complex optical equipment. Channel coding, such as LDPC, can reduce crosstalk between modes, whether under strong turbulence or weak turbulence. Because no optical equipment is required, MIMO equalization and channel coding are more suitable for the OAM waves in the millimeter band. In order to find the better mitigation method in the millimeter band, comparing MIMO equalization and channel coding will be the future research direction of this paper.

REFERENCES

[1] A. M. Yao and M. J. Padgett, "Orbital angular momentum: Origins, behavior and applications," *Adv. Opt. Photon.*, vol. 3, no. 3, pp. 161–204, Jun. 2011.

[2] R. Niemiec, C. Brousseau, K. Mahdjoubi, O. Emile, and A. Ménard, "Characterization of an OAM flat-plate antenna in the millimeter frequency band," *IEEE Antennas Wireless Propag. Lett.*, vol. 13, pp. 1011–1014, 2014.

[3] L. A. Rusch, M. Rad, K. Allahverdyan, I. Fazal, and E. Bernier, "Carrying data on the orbital angular momentum of light," *IEEE Commun. Mag.*, vol. 56, no. 2, pp. 219–224, Feb. 2018.

[4] F. Zhang and Y. Zhu, "Spectrally efficient free-space optical communications employing orbital angular momentum multiplexing," in *Proc. Prog. Electromagn. Res. Symp. (PIERS)*, Shanghai, China, 2016, p. 4873.

[5] R. Tudor, M. Kusko, M. Mihailescu, and C. Kusko, "Free space optical communications system with helical beams," in *Proc. Adv. Wireless Opt. Commun. (RTUWO)*, Riga, Latvia, 2015, pp. 207–210.

[6] C. Kai, P. Huang, H. Zhou, Z. Guo, and F. Shen, "Orbital angular momentum shift keying based optical communication system," *IEEE Photon. J.*, vol. 9, no. 2, Apr. 2017, Art. no. 7902510.

[7] Q. Tian, L. Zhu, Q. Zhang, B. Liu, X. Xin, and Y. Wang, "The propagation properties of a longitudinal orbital angular momentum multiplexing system in atmospheric turbulence," *IEEE Photon. J.*, vol. 10, no. 1, Feb. 2018, Art. no. 7900416.

[8] Y. Chen, S. Huang, and M. Safari, "Orbital angular momentum multiplexing for free-space quantum key distribution impaired by turbulence," in *Proc. 14th Int. Wireless Commun. Mobile Comput. Conf. (IWCMC)*, Limassol, Cyprus, 2018, pp. 636–641.

[9] M. Li, M. Cvijetic, Z. Yu, and Y. Takashima, "Evaluation of channel capacity of the OAM-based FSO links with a precise assessment of turbulence impact," in *Proc. Conf. Lasers Electro-Opt. (CLEO)-Laser Sci. Photonic Appl.*, San Jose, CA, USA, 2014, pp. 1–2.

[10] X. Sun and I. B. Djordjevic, "Physical-layer security in orbital angular momentum multiplexing free-space optical communications," *IEEE Photon. J.*, vol. 8, no. 1, Feb. 2016, Art. no. 7901110.

[11] J. A. Anguita, M. A. Neifeld, and B. V. Vasic, "Turbulence-induced channel crosstalk in an orbital angular momentum-multiplexed free-space optical link," *Appl. Opt.*, vol. 47, no. 13, pp. 2414–2429, May 2008.

[12] J. Zhou, J. Zong, and D. Liu, "The higher order statistics of OAM modal amplitudes under atmosphere turbulence," *IEEE Photon. Technol. Lett.*, vol. 28, no. 23, pp. 2653–2656, Dec. 1, 2016.

[13] Y. Jiang, S. Wang, H. Tang, and J. Zhang, "Spiral spectrum of Laguerre–Gaussian beam propagation in non-Kolmogorov turbulence," *Opt. Commun.*, vol. 303, pp. 38–41, Aug. 2013.

[14] Y. Yuan, T. Lei, X. Weng, L. Du, X. Yuan, and S. Gao, "The orbital angular momentum spreading for cylindrical vector beams in turbulent atmosphere," *IEEE Photon. J.*, vol. 9, no. 2, Apr. 2017, Art. no. 6100610.

[15] Y.-X. Zhang, Y.-G. Wang, J.-Y. Wang, J.-J. Jia, and J.-C. Xu, "Orbital angular momentum crosstalk of single photons propagation in a slant non-Kolmogorov turbulence channel," *Opt. Commun.*, vol. 384, pp. 1132–1138, Mar. 2011.

[16] Z. Zhang, Y. Yuan, J. Cang, H. Wu, and X. Zhang, "An orbital angular momentum-based in-band full-duplex communication system and its mode selection," *IEEE Commun. Lett.*, vol. 21, no. 5, pp. 1183–1186, May 2017.

[17] D. Shin, E. Park, J. Myung, J. Kang, and J. Kang, "Identification of non-ideal receiver condition for orbital angular momentum transmission," in *Proc. IEEE 79th Veh. Technol. Conf. (VTC Spring)*, Seoul, South Korea, May 2014, pp. 1–5.

[18] J.-B. Kim and M. S. Song, "Impact of inter-mode interference on BER performance of orbital angular momentum based radio communications," in *Proc. Int. Conf. Inf. Commun. Technol. Converg.*, Jeju, South Korea, 2016, pp. 969–972.

[19] Y. Ren, L. Li, G. Xie, Y. Yan, Y. Cao, H. Huang, N. Ahmed, Z. Zhao, P. Liao, C. Zhang, G. Caire, A. F. Molisch, M. Tur, and A. E. Willner, "Line-of-sight millimeter-wave communications using orbital angular momentum multiplexing combined with conventional spatial multiplexing," *IEEE Trans. Wireless Commun.*, vol. 16, no. 5, pp. 3151–3161, May 2017.

[20] Y. Yuan, Z. Zhang, H. Wu, C. Zhong, and J. Cang, "Capacity analysis of UCA-based OAM multiplexing communication system," in *Proc. Int. Conf. Wireless Commun. Signal Process. (WCSP)*, Nanjing, China, 2015, pp. 1–5.

[21] Z. Zhang, S. Zheng, X. Jin, H. Chi, X. Zhang, and Y. Chen, "The capacity gain of orbital angular momentum based multiple-input-multiple-output system," *Sci. Rep.*, vol. 6, May 2016, Art. no. 25418.

[22] X. Ge, R. Zi, X. Xiong, Q. Li, and L. Wang, "Millimeter wave communications with OAM-SM scheme for future mobile networks," *IEEE J. Sel. Areas Commun.*, vol. 35, no. 9, pp. 2163–2177, Sep. 2017.

[23] S. Gao, W. Cheng, Z. Li, and H. Zhang, "High-efficient beam-converging for UCA based radio vortex wireless communications," in *Proc. IEEE/CIC Int. Conf. Commun. China (ICCC)*, Qingdao, China, Oct. 2017, pp. 1–6.

[24] L. Wang, X. Ge, R. Zi, and C.-X. Wang, "Capacity analysis of orbital angular momentum wireless channels," *IEEE Access*, vol. 5, pp. 23069–23077, 2017.

[25] J. Xu, "Generation of Laguerre–Gaussian modes by aperture or array sources," *IEEE Trans. Antennas Propag.*, vol. 67, no. 1, pp. 415–429, Jan. 2019.

[26] J. Chen, X. Ge, and Q. Ni, "Coverage and handoff analysis of 5G fractal small cell networks," *IEEE Trans. Wireless Commun.*, to be published.

[27] R. W. Mcmillan, "Intensity and angle-of-arrival effects on microwave propagation caused by atmospheric turbulence," in *Proc. IEEE Int. Conf. Microw., Commun., Antennas Electron. Syst.*, Tel-Aviv, Israel, May 2008, pp. 1–10.

[28] X. Ge, X. Tian, G. Mao, T. Han, and Y. Qiu, "Small-cell networks with fractal coverage characteristics," *IEEE Trans. Commun.*, vol. 66, no. 11, pp. 5457–5469, Nov. 2018.

[29] R. J. Hill, R. A. Bohlander, S. F. Clifford, R. W. McMillan, J. T. Priestly, and W. P. Schoenfeld, "Turbulence-induced millimeter-wave scintillation compared with micrometeorological measurements," *IEEE Trans. Geosci. Remote Sens.*, vol. 26, no. 3, pp. 330–342, May 1988.

[30] C. Chen, H. Yang, Y. Lou, and S. Tong, "Changes in orbital-angular-momentum modes of a propagated vortex Gaussian beam through weak-to-strong atmospheric turbulence," *Opt. Express*, vol. 24, no. 7, pp. 6959–6975, Apr. 2016.

[31] L. C. Andrews and R. L. Phillips, *Laser Beam Propagation Through Random Media*, 2nd ed. Bellingham, WA, USA: SPIE Press, 2005.

[32] X.-L. Yin, C. Xu, J.-J. Han, X.-J. Xin, L. Li, C.-X. Yu, and J. Hao, "Effects of atmosphere turbulence on the purity of light carrying orbital angular momentum employing Zernike polynomials method," in *Proc. 13th Int. Conf. Opt. Commun. Netw. (ICOCN)*, Suzhou, China, 2014, pp. 1–4.

[33] X. Ge, Y. Sun, H. Gharavi, and J. Thompson, "Joint optimization of computation and communication power in multi-user massive MIMO systems," *IEEE Trans. Wireless Commun.*, vol. 17, no. 6, pp. 4051–4063, Jun. 2018.

[34] A. Amphawan, S. Chaudhary, and V. Chan, "Optical millimeter wave mode division multiplexing of LG and HG modes for OFDM Ro-FSO system," *Opt. Commun.*, vol. 431, pp. 245–254, Jan. 2018.

[35] C. Paterson, "Atmospheric turbulence and orbital angular momentum of single photons for optical communication," *Phys. Rev. Lett.*, vol. 94, no. 15, Apr. 2005, Art. no. 153901.

[36] Z. Qu and I. B. Djordjevic, "Two-stage cross-talk mitigation in an orbital-angular-momentum-based free-space optical communication system," *Opt. Lett.*, vol. 42, no. 10, pp. 3125–3128, Aug. 2017.

[37] H. Huang, Y. Cao, G. Xie, Y. Ren, Y. Yan, C. Bao, N. Ahmed, M. A. Neifeld, S. J. Dolinar, and A. E. Willner, "Crosstalk mitigation in a free-space orbital angular momentum multiplexed communication link using 4 × 4 MIMO equalization," *Opt. Lett.*, vol. 39, no. 15, pp. 4360–4363, Aug. 2014.

[38] Y. Ren, G. Xie, H. Huang, L. Li, N. Ahmed, Y. Yan, M. P. J. Lavery, R. Bock, M. Tur, M. A. Neifeld, R. W. Boyd, J. H. Shapiro, and A. E. Willner, "Turbulence compensation of an orbital angular momentum and polarization-multiplexed link using a data-carrying beacon on a separate wavelength," *Opt. Lett.*, vol. 40, no. 10, pp. 2249–2252, May 2015.

[39] X. Ge, "Ultra-reliable low-latency communications in autonomous vehicular networks," *IEEE Trans. Veh. Technol.*, vol. 68, no. 5, pp. 5005–5016, May 2019.

[40] Z. Qu and I. B. Djordjevic, "500 Gb/s free-space optical transmission over strong atmospheric turbulence channels," *Opt. Lett.*, vol. 41, no. 14, pp. 3285–3288, Jul. 2016.

[41] I. S. Gradshteyn, I. M. Ryzhik, *Table of Integrals, Series, and Products*, 6th ed. New York, NY, USA: Academic, 2000.

[42] Y. Gong, R. Wang, B. Zhang, N. Wang, N. Li, P. Wang, and Y. Deng, "Generation and transmission of OAM-carrying vortex beams using circular antenna array," *IEEE Trans. Antennas Propag.*, vol. 65, no. 6, pp. 2940–2949, Jun. 2017.

[43] S. M. Mohammadi, L. K. S. Daldorff, R. L. Karlsson, and J. E. S. Bergman, "Orbital angular momentum in radio—A system study," *IEEE Trans. Antennas Propag.*, vol. 58, no. 2, pp. 565–572, Feb. 2010.

HANQIONG LOU received the B.E. degree in communication engineering from the Huazhong University of Science and Technology (HUST), Wuhan, China, in 2017, where she is currently pursuing the M.S. degree. Her research interest mainly includes the orbital angular momentum (OAM) technology.

XIAOHU GE (M'09–SM'11) received the Ph.D. degree in communication and information engineering from the Huazhong University of Science and Technology (HUST), China, in 2003. He was a Researcher with Ajou University, South Korea, and the Politecnico Di Torino, Italy, from January 2004 to October 2005. He has been with HUST, since November 2005, where he is currently a Full Professor with the School of Electronic Information and Communications. He is also an Adjunct Professor with the Faculty of Engineering and Information Technology, University of Technology Sydney (UTS), Australia. He has published about 200 articles in refereed journals and conference proceedings and has been granted about 25 patents in Chinese. His research interests include mobile communications, traffic modeling in wireless networks, green communications, and interference modeling in wireless communications. He serves as the IEEE Distinguished Lecturer and an Associate Editor for IEEE Access, the IEEE Wireless Communications, and the IEEE Transactions on Vehicular Technology.

QIANG LI (M'16) received the B.Eng. degree in communication engineering from the University of Electronic Science and Technology of China (UESTC), Chengdu, China, in 2007, and the Ph.D. degree in electrical and electronic engineering from Nanyang Technological University (NTU), Singapore, in 2011. From 2011 to 2013, he was a Research Fellow with NTU. Since 2013, he has been an Associate Professor with the Huazhong University of Science and Technology (HUST), Wuhan, China. From March 2015 to June 2015, he was a Visiting Scholar with The University of Sheffield, Sheffield, U.K. His current research interests include the next-generation mobile communications, software-defined networking, cooperative edge caching, cognitive radios/spectrum sharing, simultaneous wireless information and power transfer, wireless cooperative communications, and full-duplex relays.